Renewable and Sustainable Energy Reviews 21 (2013) 131–141

Contents lists available at SciVerse ScienceDirect

Renewable and Sustainable Energy Reviews

journal homepage: www.elsevier.com/locate/rser

Assessment of offshore wind energy at Younggwang in Korea

Myung Eun Lee [a], Gunwoo Kim [b], Shin-Taek Jeong [c,*], Dong Hui Ko [c], Keum Seok Kang [d]

[a] Department of Civil and Environmental Engineering, Seoul National University, Seoul 151-742, Republic of Korea
[b] Department of Ocean Civil & Plant Construction Engineering, Mokpo National Maritime University, Mokpo, Jeollanamdo 530-729, Republic of Korea
[c] Department of Civil and Environmental Engineering, Wonkwang University, Iksan, Jeollabukdo 570-749, Republic of Korea
[d] KEPCO Research Institute, Daejeon 305-380, Republic of Korea

ARTICLE INFO

Article history:
Received 15 October 2012
Received in revised form
29 December 2012
Accepted 29 December 2012
Available online 26 January 2013

Keywords:
Offshore wind energy
HEMOSU-1
Weibull distribution
Wind power potential
Wind turbine

ABSTRACT

This study aimed to assess the potential of offshore wind power generation at Younggwang in Korea which is candidate site of the offshore wind farm planned to be constructed till 2019. Toward this purpose, offshore meteorological tower called HEMOSU-1 was installed and has collected the wind and other meteorological data since October, 2010. The Weibull model was fitted to the frequency distribution of data and it was found that the measured data fit well to Weibull models with properly estimated parameters. Winter was found to be the best for harnessing wind energy because of the high wind speeds and consistent wind direction from the northwestern Siberian high. An assessment of the available power density at the height of 97.35 m indicates that there is an abundant wind power density—averaged to be 429.20 W/m^2 annually and 509.97 W/m^2 during winter. After testing various commercial wind turbines with rated power in the range of 3–7 MW, REpower 5 M was chosen for the analysis of installation at the wind farm in Younggwang. It was found that the annual energy production is expected to be about 7096 GWh/yr.

Contents

1. Introduction

Renewable energy is attracting rapidly increasing attention worldwide. This interest has been precipitated by increasing environmental problems such as global warming and by the depletion of fossil fuels, accompanied by unstable oil prices. In Korea where the production of electric energy was mainly dependent on fossil fuels for a long time, there is also an increasing interest in renewable energy. The necessity of having a stable energy supply was first realized after the two oil crises of the 1970s. A systematic plan for developing national renewable energy began in the 1980s, accompanied by a social recognition of the importance of having a stable energy supply. Initially, the hydropower obtained from dams was the primary resource for

* Corresponding author. Tel.: +82 63 850 6714; fax: +82 63 850 6792.
E-mail address: stjeong@wonkwang.ac.kr (S.-T. Jeong).

1364-0321/$ - see front matter © 2013 Elsevier Ltd. All rights reserved.
http://dx.doi.org/10.1016/j.rser.2012.12.059

renewable energy production. However, because suitable sites for the dam construction were limited and dam construction gave rise to negative environmental side effects, the construction of hydropower dams has not progressed. Although wind power is a typical renewable and sustainable energy source, free from pollutants such as carbon dioxide and radioactive substances, it has not been considered as a major source for national energy supply in Korea. However, due to increasing demands for renewable energy and recent developments in technology, the wind power becomes one of the most promising renewable energy resources.

1.1. Situation of Korean wind power

Due to the strong effect of East Asian monsoon, Korea has four distinct seasons: spring, summer, autumn, and winter. The contrast between winter and summer is considerable—winter is bitterly cold, influenced primarily by the Siberian air mass from the northwest, whereas summer is hot and humid due to the maritime Pacific high of the southeast region. Therefore, there is large fluctuation in the national electric power demand; the peak demand occurs in summer or winter. Recently, due to the frequent occurrence of far below—average temperature in winter associated with the abnormal climate change worldwide, handling the steep growth of electricity demand in winter in Korea became a matter of priority. Especially between 2010 and 2011, the maximum power demand increased in winter due to the abnormally intense cold wave, whereas the annual maximum demand usually occurred in summer before 2008. The most recent maximum electric demand was recorded to be 73,140 MW on January 17, 2011 and the corresponding possible maximum electric supply was 77,180 MW; thus, the electric power reserve rate was only 5.5% at that time. The severely cold temperature leads to a significant increase in the use of electric heating that exceeds the amount of air-conditioning used in summer, because of relatively large cost of heating fuels. Therefore, it is necessary to prepare measures to deal with future increase in demand in winter associated with the climate change.

The first record of a wind turbine in Korea is that of a 2.2 kW—turbine installed in Hwasung City in 1975. In 1992, a 250 kW wind turbine was installed on Jeju island; it was the first turbine to be connected to the power grid system in Korea. The first large-scale wind energy farm was established in Yeongdeok District in 2005; it had an installation capacity of 39.6 MW in 2005. Thereafter, the construction of the wind energy farms rapidly increased, due to the economical growth of Korea which induced the interest in sustainable development of the country. By 2009, the total installed capacity was increased up to 342 MW. The accumulated installed capacity of wind power plants from 2004 to 2009 is presented in Fig. 1. It can be seen that the capacity drastically increased in 2006 and 2009. Most of wind energy farms in Korea constructed during this period have only been built onshore locations, in spite of the high energy potential of offshore wind power plants because of the lack of detailed information on offshore wind energy plants and other technical problems. However, there has been a continuous effort to find the proper site for a large-scale offshore wind farm by Korean government. As a result, the construction of an offshore wind energy farm is planned in Younggwang as introduced in the next section.

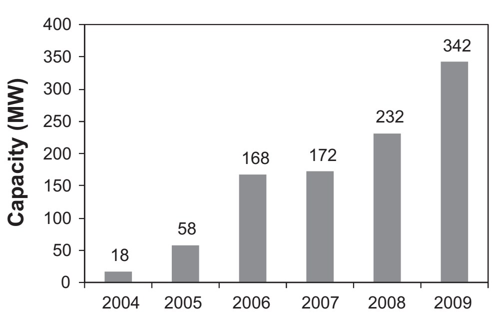


Fig. 1. Accumulate total installed capacity in South Korea.



Fig. 2. Map of wind energy farm locations.

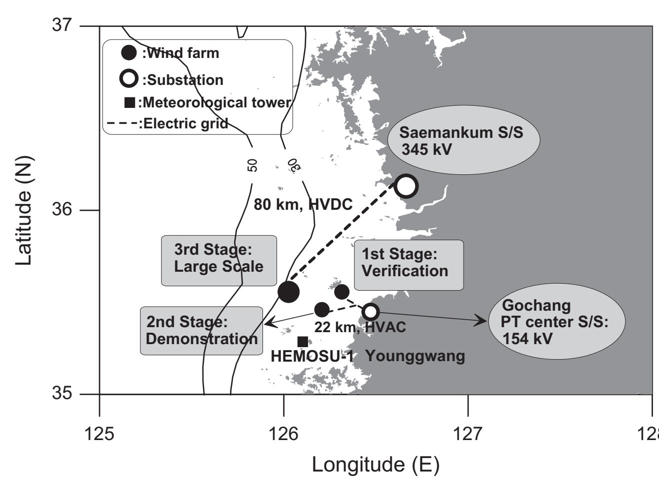


Fig. 3. Locations of offshore wind farm and electric grids to substations with bathymetry contour for water depth (m).

Table 1
The impact of depth and distance on costs [3].

Water depth (m)	Distance from shore (km)							
	0–10	10–20	20–30	30–40	40–50	50–100	100–200	> 200
10–20	1	1.02	1.04	1.07	1.09	1.18	1.41	1.60
20–30	1.07	1.09	1.11	1.14	1.16	1.26	1.50	1.71
30–40	1.24	1.26	1.29	1.32	1.34	1.46	1.74	1.98
40–50	1.40	1.43	1.46	1.49	1.52	1.65	1.97	2.23

1.2. Offshore wind energy farm in Younggwang, Korea

The Korean government is planning to construct a 2500 MW-class offshore wind farm by 2019 along the south-western coast. The selected site is in the Younggwang region (Fig. 2), where the wind is of Class 3 (6.9–7.5 m/s), the mean sea water depth is 20 m, and the distance of the site from the substation is about 15 km. The outline of the strategic plan for the establishment of this offshore wind energy farm is divided into three phases:

- First stage: by 2014, construct a 100 MW test bed for verification.
- Second stage: by 2016, construct a 400 MW demonstration site.
- Third stage: by 2019, establish a 2000 MW large-scale wind farm.

The private and public sectors will invest a total of 10.2 trillion won (92.7 billion USD) to build a large-scale offshore wind farm with 2500 MW. The location of the wind energy farm, i.e., Younggwang, was selected after examining the Korea National Wind Map, which was established by using the RDAPS (Regional Data Assimilation and Prediction System) data with a grid size of 3 km and a frequency of 3 h from 2005 to 2007 [1]. RDAPS is an operational weather forecast model based on the MM5 model [2]. The roadmap of the offshore wind farm around Younggwang is presented in Fig. 3. In the first and second stages, test bed will be connected to Gochang substation with grid of 154 kV—HVAC by using domestic technology. In the third stage, the large-scale wind farm will be connected to Saemankum substation of 345 kV using HVDC transmission.

The costs for offshore wind generation are usually much higher than for onshore wind farms because of the additive cost for transmission grid to substations inland and their maintenance cost against corrosion and meteorological damage. The level of the cost premium of offshore wind relative to onshore wind stations depends on factors including water depth and distance from shore. EEA [3] provided the adjustment factor by which investment and installation costs should be multiplied for deeper water and greater distance as shown in Table 1. According to Fig. 3, the location of wind farm of the third stage in plan around Younggwang is inside 30 m isobaths and the distance to Saemankum substation is 80 km, which means its cost premium factor is about 1.26 in Table 1. There is another economic factor to be considered for the construction of wind farm in the offshore of Younggwang because of the flimsy ground of sea bed around this site. On the flimsy sea bed, multi-pile structure such as jacket type or pile cap is preferred to mono-pile with gravity type as the support structure of wind tower, and the cost of multi-pile structure is generally larger than mono-pile. Providing 3 MW-turbine on the 15 m water depth, a jacket type structure results in more cost than pile cap through the economic evaluation [4]. Therefore, pile cap method for multi-pile support is recommended for the construction of wind farm.

In addition to economic feasibility of wind farm, there are several environmental factors to be considered for the construction of wind farm around Younggwang. The south-western part of Korea, in which Younggwang is located, is on the East Asian–Australasian Flyway which is the one of the important pathways of a migrant. Various kinds of birds use the coastal region of south-western part of Korea as their route or settlement. Thus, it is necessary to evaluate the effect of the offshore wind farm on the moving path of birds through this region. Furthermore, the south-western coastal region is also well-known for its shallow water depth and tidal flat with great tidal range. Due to this geographical characteristic, a fishery and aquaculture industry is the main source of income in this area. Therefore, the research for the preservation of fishing ground here and the agreement with fishermen with respect to fishery activity is prerequisite before the construction of wind farm. These environmental problems mentioned above will be testified after construction of the test bed for verification in the first stage.

Towards the final stage of wind farm construction in Younggwang region, deficient infrastructure for electric grid connection in the south-western part of Korea also has to be resolved. After demonstration of the second stage, large-scale offshore wind farm is planned to be connected to Saemankum substation using HVDC. However, it is not possible to connect only with domestic technical skill, and construction by a foreign company results in relatively high cost and low contribution to national technical level. Furthermore, government will continue to expand the facility of Younggwang

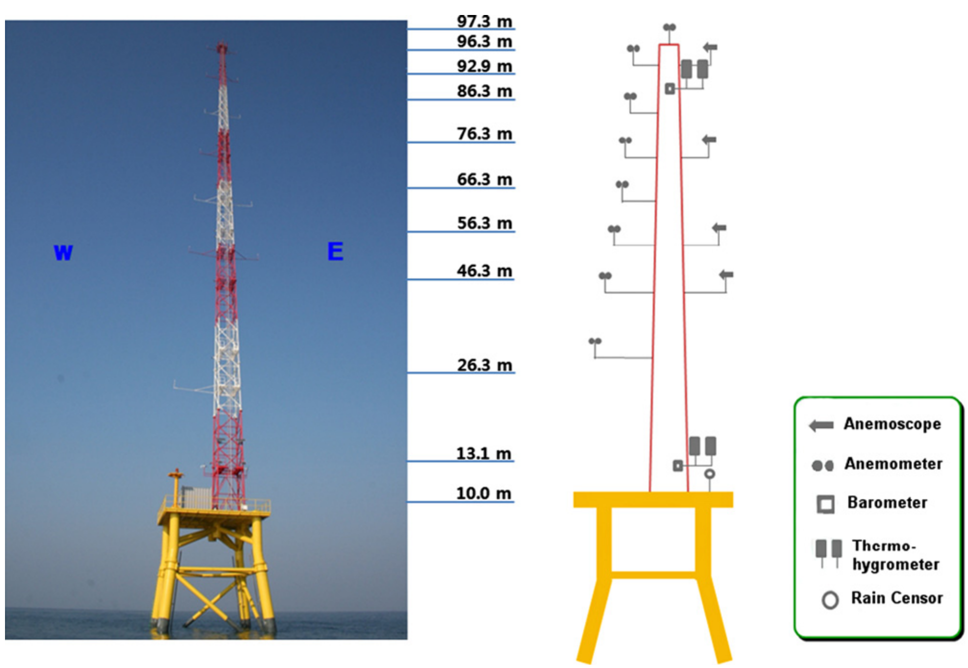


Fig. 4. HEMOSU-1 offshore meteorological unit.

Table 2
Description of facilities in HEMOSU-1.

El. (m) (above MSL)	Equipment	El. (m) (above MSL)	Equipment
97.35	Anemometer	56.31	Anemoscope, anemometer
96.31	Anemoscope, anemometer	46.31	Anemoscope, anemometer
92.85	Barometers, thermo-hygrometers	26.31	Anemometer
86.31	Anemometer	13.05	Barometers, thermo-hygrometers
76.31	Anemoscope, anemometer	11.72	Rainfall sensor
66.31	Anemometer	10.02	Deque

Table 3
Annual mean, standard deviation, and maximum wind speed of measurement in 2011 by HEMOSU-1.

Height (m)	Mean (m/s)	Standard deviation (m/s)	Max. 10 min average (m/s)
97.350	7.122	3.907	30.570
96.310	6.942	3.900	30.760
86.310	6.853	3.750	30.120
76.310	6.752	3.703	29.760
66.310	6.818	3.718	29.970
56.310	6.505	3.608	28.850
46.310	6.394	3.451	27.950
26.310	6.081	3.301	26.730

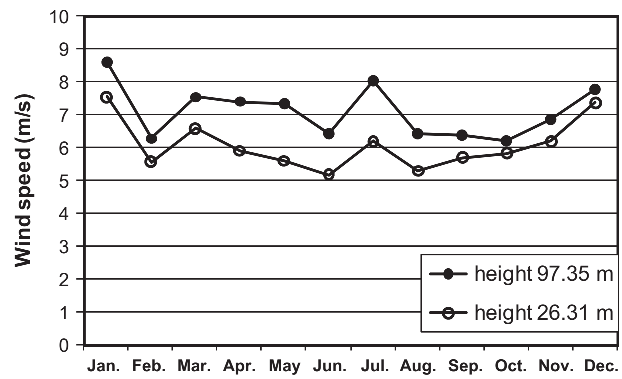


Fig. 5. Annual variation of wind speed in Younggwang.

Table 4
Seasonal mean, standard deviation, and maximum wind speed of measurement in 2011—winter by HEMOSU-1.

Height (m)	Mean (m/s)	Std. deviation (m/s)	Max. 10 min average (m/s)
97.350	7.614	3.856	24.460
96.310	7.413	3.878	24.580
86.310	7.326	3.684	24.070
76.310	7.238	3.667	23.860
66.310	7.362	3.734	24.060
56.310	6.999	3.666	22.930
46.310	7.000	3.543	22.220
26.310	6.874	3.514	21.380

Table 5
Estimated annual Weibull parameters.

Height	2011		2011—winter	
	k	*c*	*k*	*c*
97.350	1.919	8.029	2.093	8.597
96.310	1.870	7.819	2.021	8.367
86.310	1.924	7.725	2.109	8.272
76.310	1.920	7.611	2.093	8.173
66.310	1.932	7.688	2.090	8.312
56.310	1.897	7.330	2.018	7.899
46.310	1.954	7.211	2.095	7.904
26.310	1.942	6.858	2.073	7.761

offshore wind farm after completion of the third stage. The capacity of existing grid facility in this area is far from sufficient to manage larger than a 1500 MW-power plant. Extensive supplement of electrical grid in south-western region of Korea should be carried out for the successful settlement of power production of the Younggwang large-scale offshore wind farm.

This study provides the assessment of the possible energy production by the wind farm at Younggwang based on the wind data of 1 yr in 2011 measured near the candidate site.

2. Analysis of wind data

2.1. Meteorological mast description

The wind measurement at a specific location can effectively represent the wind characteristics of the site under consideration. For this reason, KEPCO (Korea Electric Power Corporation) installed the HEMOSU-1 (Herald of Meteorological and Oceanographic Special Unit-1), an offshore tower (Fig. 4) at 126° 07′ 45.30″ E and 35° 27′ 55.17″ N, in order to measure the wind data in the Younggwang region. The height of the tower is about 100 m above mean sea level, and its equipments and their elevations are depicted in Table 2 and Fig. 4. The sampling rate of data is 0.3 s and they are averaged at a regular interval of 10 min.

2.2. Wind speed distribution

The statistical information of annual data is presented in Table 3. The annual mean of wind speed was observed as 6.081–7.122 m/s which increases as the observation elevation becomes high. To investigate the winter data, observation data during January, February, and December were separately collected, and the statistical characteristics during these months are presented in Table 4. The mean wind speed in winter was about 0.5 m larger than the annual mean wind speed.

To investigate the annual variation of wind speed, the monthly mean wind speeds of year 2011 are plotted in Fig. 5. The maximum mean wind speed of 8.609 and 7.539 m/s was observed in January at the top and bottom observation elevations of 97.35 m and 26.31 m, whereas the minimum mean wind speed of 6.202 and 5.158 m/s was observed in October and June, respectively. The annual fluctuation range of wind speed was about 2.4 m/s between maximum and minimum monthly averaged wind speed.

To evaluate the wind energy potential of a site, it is convenient to introduce the probability distribution of the site's wind speed. Weibull distribution has been generally used in many literatures

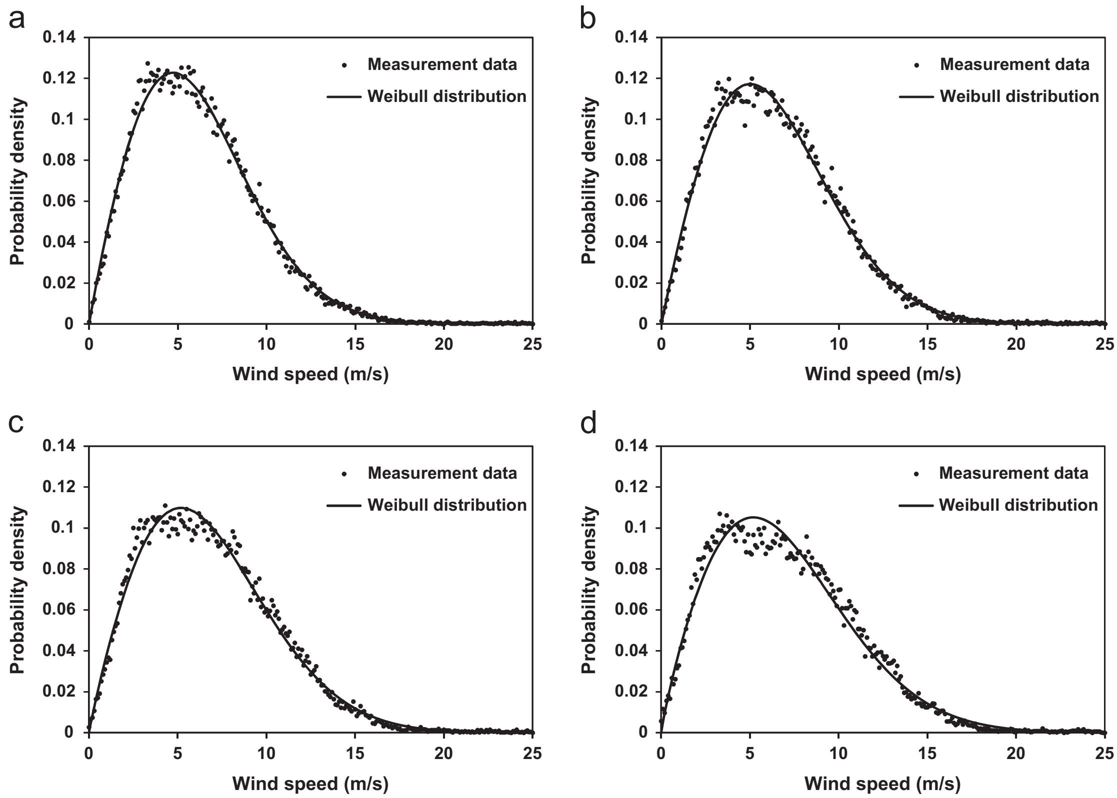


Fig. 6. Histograms of wind speed data and estimated Weibull distributions in 2011: (a) 26.31 m, (b) 46.31 m, (c) 76.31 m, (d) 96.31 m.

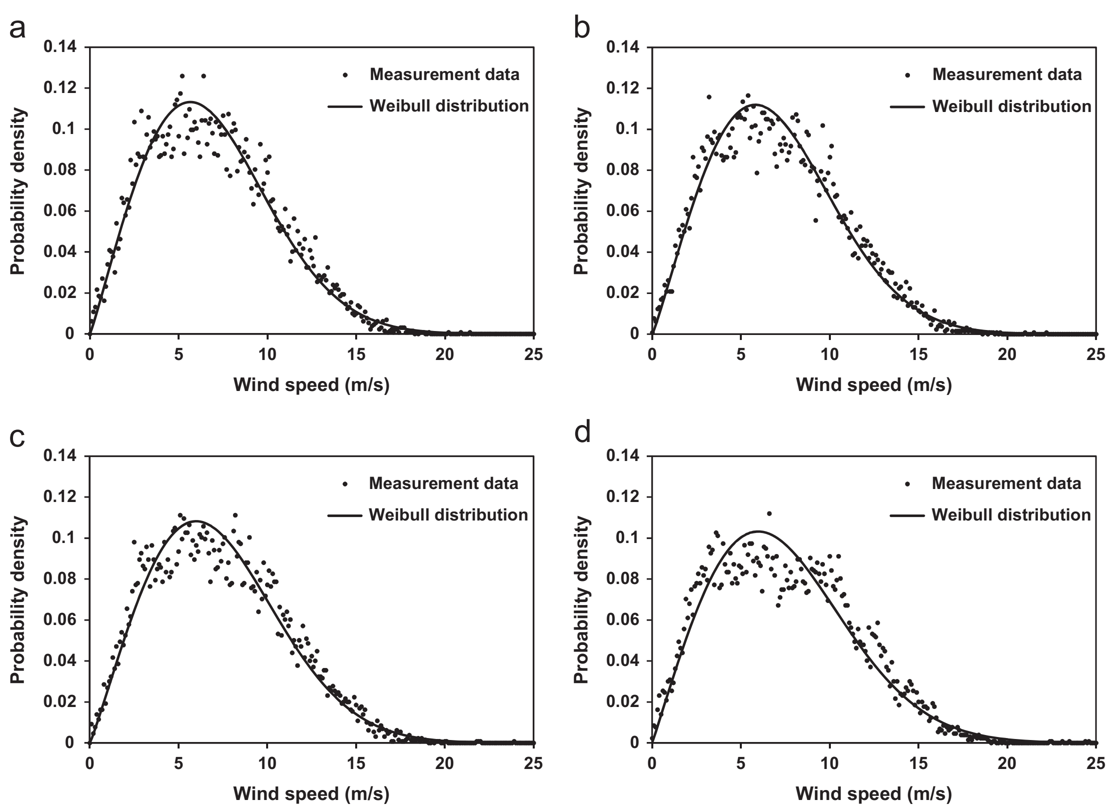


Fig. 7. Histograms of wind speed data and estimated Weibull distributions in 2011—winter: (a) 26.31 m, (b) 46.31 m, (c) 76.31 m, (d) 96.31 m.

to express the wind speed frequency distribution of a specific location [5–10]. In terms of Weibull distribution, the probability density function for the wind speed V is expressed as

$$f(V)=\frac{k}{c}\cdot\left(\frac{V}{c}\right)^{k-1}\cdot\exp\left[-\left(\frac{V}{c}\right)^{k}\right] \tag{1}$$

where k is the dimensionless shape parameter, and c is the scale parameter. The cumulative distribution function, which gives the probability that the wind velocity, is equal or lower than V is

$$F(V)=1-\exp\left[-\left(\frac{V}{c}\right)^{k}\right] \tag{2}$$

Analytical or empirical methods can be used for the parameter estimation, and the method of Justus et al. [11,12] was used in this study as

$$k=\left(\frac{\sigma}{\overline{V}}\right)^{-1.086} \tag{3}$$

$$c=\frac{\overline{V}k^{2.6674}}{0.184+0.816k^{2.73855}} \tag{4}$$

where $\overline{V}$ and σ are the mean and the standard deviation of the observation data V, respectively, such as

$$\overline{V}=\sum_{i=1}^{N}V_i \tag{5}$$

$$\sigma=\sqrt{\sum_{i=1}^{N}(V_i-\overline{V})^2/(N-1)} \tag{6}$$

where V_i is the wind speed averaged for every 10 min, and N is the total number of data for a given duration.

The parameters k and c were obtained from the annual and winter data, respectively. Estimated parameters of each observation height for annual and winter are shown in Table 5. The maximum k is obtained as 2.109 at 86.31 m in winter, whereas the maximum c was obtained to be 8.597 at 97.35 m in winter. The both adjusted Weibull models of annual and winter data approach to the Rayleigh distribution for $k=2$. However, k of annual distribution is smaller than 2 whereas that of winter slightly exceeds over 2. The larger values of k in winter imply that the wind speed distribution in winter is less positively skewed than those of annual data.

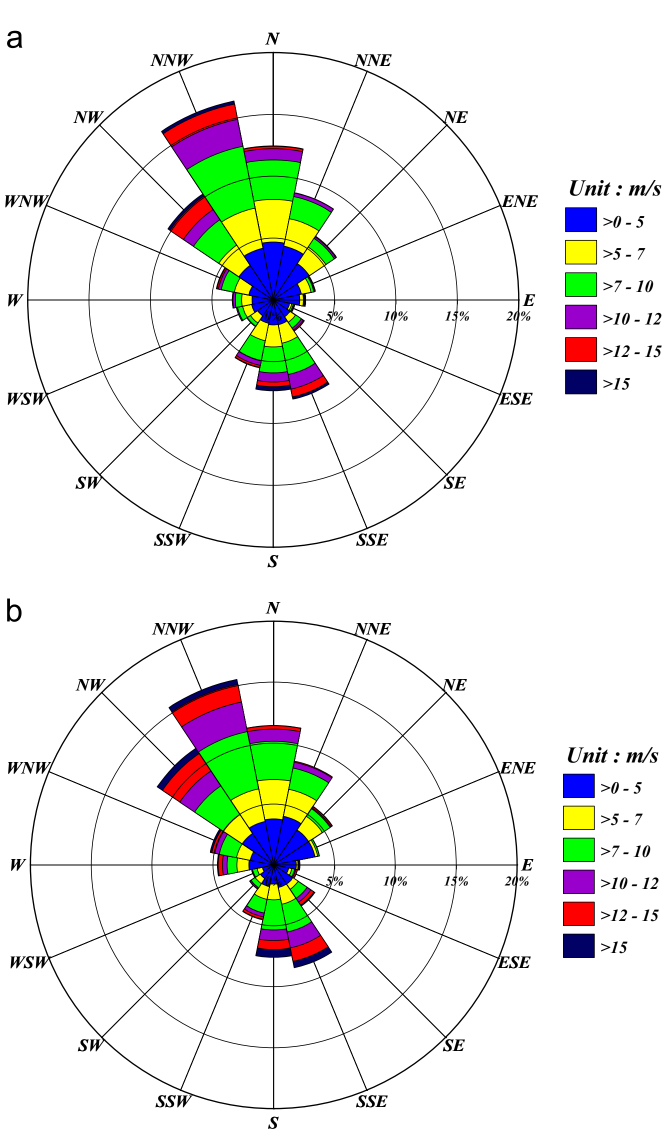


Fig. 8. Wind rose diagram of measurement in 2011: (a) 46.31 m, (b) 96.31 m.

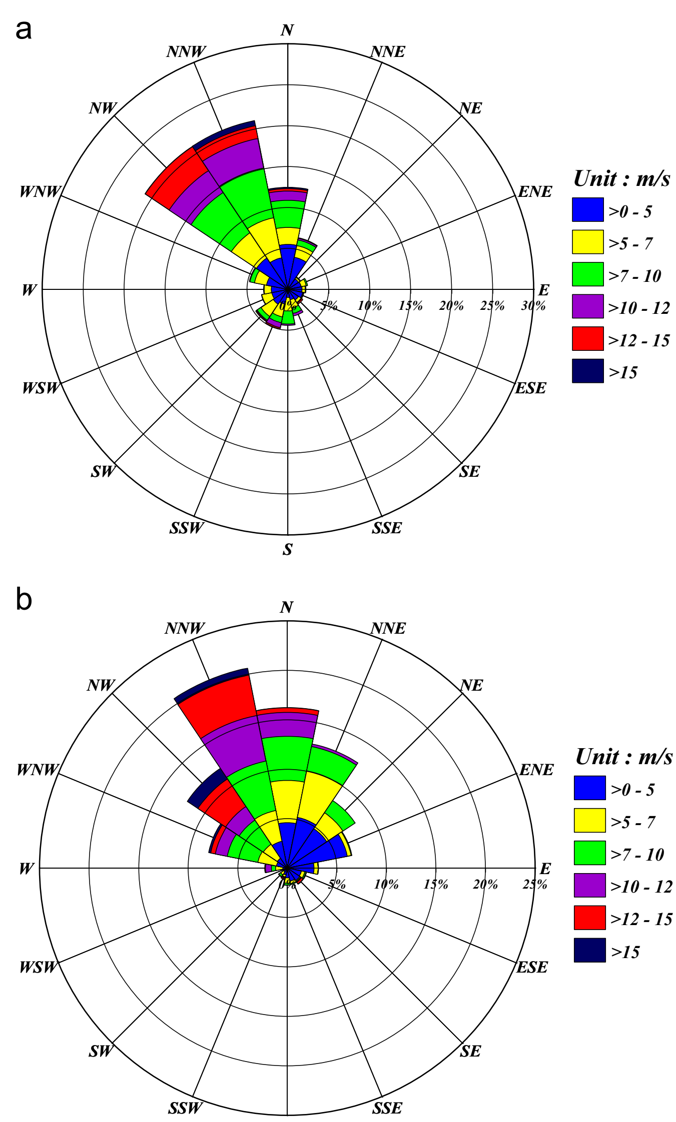


Fig. 9. Wind rose diagram of measurement in 2011—winter: (a) 46.31 m, (b) 96.31 m.

The parameter c is definitely small in the low elevations, because it is deeply related to the mean wind speed. As shown in Table 4, the decreasing rate of c in winter is smaller than that of annual distribution, which implies that the variation of wind speed is relatively small in winter season.

Figs. 6 and 7 show the wind data at elevations of 26.31, 46.31, 76.31, 96.31 m, and their corresponding Weibull distributions for the annual and winter season, respectively. Weibull seems to give a reasonable fit to observed distributions of both annual and winter data. Due to the relatively small number of the observation in winter, the histograms of measurement showed large fluctuations in the range of the middle wind speed in Fig. 7. However, the mean distribution of observation data is not largely deviated from the estimated Weibull, and it fits well especially in the high speed range.

2.3. Wind direction

It is well known that the meteorological characteristics of the Korean peninsula are dominated by the seasonal monsoon. The north-western wind induced by Siberian high is dominant throughout Korea in the winter season, while the south-southeastern wind from the Pacific high dominates in summer. In spring and autumn, the north-northeastern winds comprise a relatively large proportion of the wind, and the south-southwestern wind is added in autumn. Because Younggwang is located on the western coast of the Korean peninsula, this site is vulnerable to the influence of the winter monsoon with prevailing northwestern wind. Furthermore, the winds in winter are much stronger than those in any other season.

In the measurement of this study, wind directions were measured at four elevations: 46.31, 56.31, 76.31, 96.31 m as in Table 2. Among them, data measured at 46.31 and 96.31 m were depicted as wind roses in Figs. 8 and 9 for the annual and the winter, respectively. As shown in Fig. 8, north-northwestern (NNW) and south-southeastern (SSE) winds dominated, respectively, in winter and summer. Fig. 8 clearly shows the strong monsoon effect on the seasonal wind direction. As shown in the winter wind rose depicted in Fig. 9, the wind of NW, NNW, and N is greatly prevalent, which comprises about 54%
and 49% of the wind during the winter at 46.31 and 96.31 m, relatively.

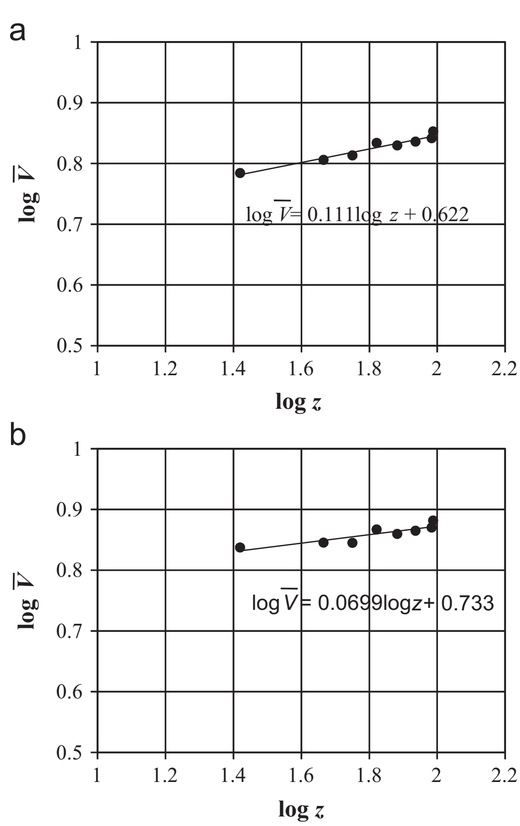


Fig. 10. Vertical profile of the measured wind speed: (a) for annually averaged data, (b) for averaged data during winter.

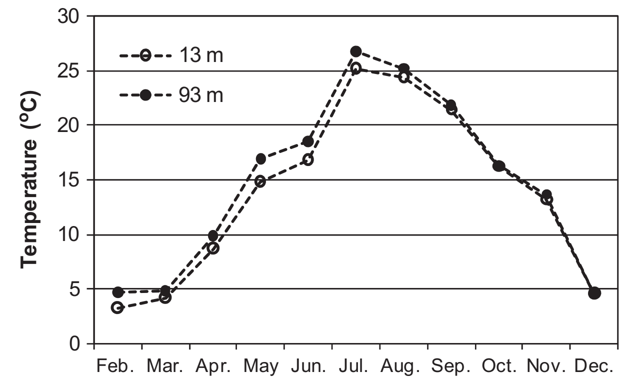


Fig. 11. Monthly mean values of temperature measured by HEMOSU-1 in 2011.

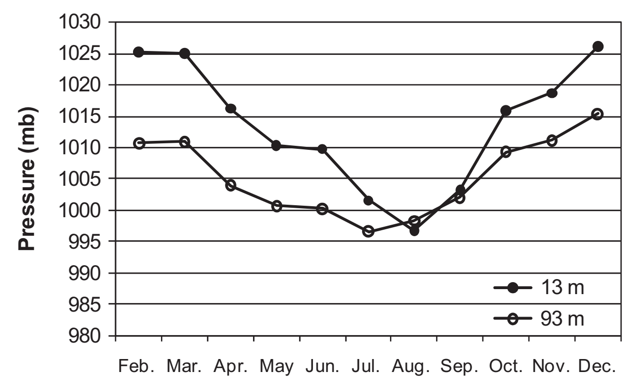


Fig. 12. Monthly mean values of atmospheric pressure measured by HEMOSU-1 in 2011.

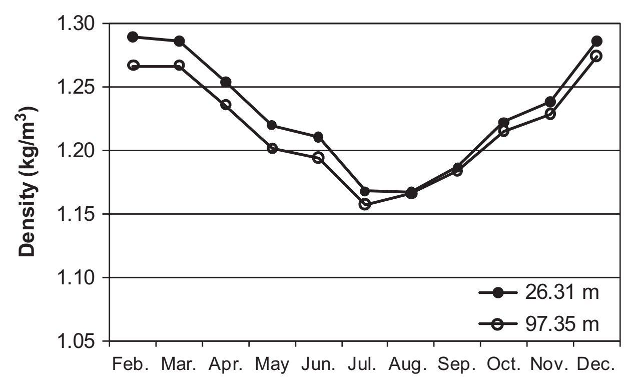


Fig. 13. Computed monthly mean values of air density of Younggwang.

2.4. Vertical wind profile

It is important to ensure the accuracy of the wind data at the level of the turbine blade. In most meteorological station, wind data are collected at a certain elevation, but we measured the

wind speed at eight different elevations, which provide the typical shape of vertical wind profile around the candidate site.

According to the literature [5,7,13,14], the most commonly used method to adjust the wind velocity at one level to another is the power law method expressed as [15,16]

$$V = V_0 \left(\frac{z}{z_0}\right)^{\beta} \tag{7}$$

where V_0 is the wind speed recorded at the anemometer height, z_0, and β is the roughness factor of the site. In this study, β was obtained by applying least square method to the linear relation between $\log z$ and $\log \overline{V}$. Fig. 10 shows the calculated $\overline{V}(z)$ at eight observation elevations in log–log axis. Vertical profile of annually averaged data was linearly approximated by β=0.111 while the profile of averaged wind during winter has gradient of β=0.0699.

2.5. Weather condition

Because of seasonal variation of prevailing air-mass, meteorological characteristics such as temperature and atmospheric pressure also show large variations for each season. Fig. 11 shows the monthly mean values of temperature measured at elevations of 13.05 and 92.85 m except for January when meteorological data were not collected. Temperature showed large variations ranging from 25.5 °C in July and 3.4 °C in February at the low elevation (13 m).

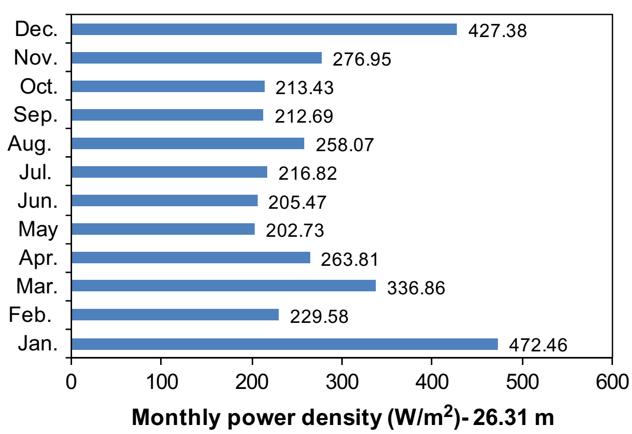


Fig. 14. Monthly power density from measurement at 26.31 m of HEMOSU-1.

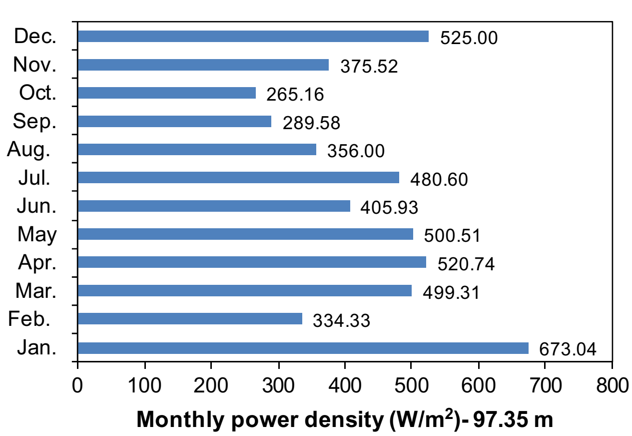


Fig. 15. Monthly power density from measurement at 97.35 m of HEMOSU-1.

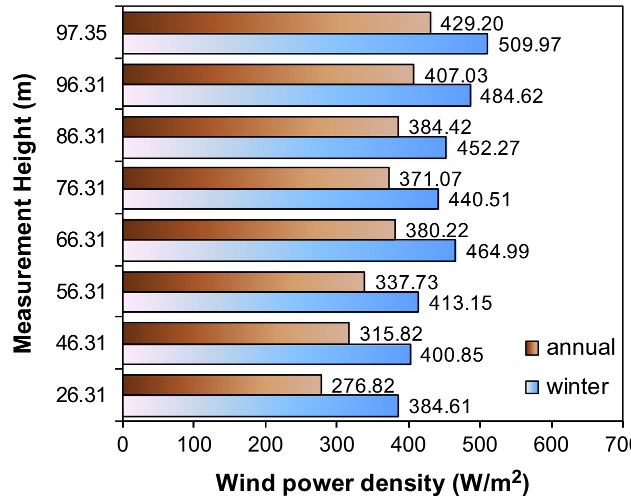


Fig. 16. Annual mean power density and seasonal mean power density in winter from measurement of HEMOSU-1.

Fig. 12 shows the monthly mean atmospheric pressures measured at 13 m and 93 m. Due to the relatively high variations of the seasonal temperature, the difference between the maximum and minimum monthly-averaged pressure at upper elevation (93 m) is observed about 27.3 mb. The vertical stratification of atmospheric pressure in summer was negligibly small, whereas the difference in pressure in February reached up to 12.7 mb.

Relatively low temperature and high pressure in winter make the wind energy potential much higher than that of other season because the air density is proportional to atmospheric pressure and inversely proportional to temperature by the following ideal gas law

$$\rho = \frac{\overline{p}}{R\overline{T}} \tag{8}$$

where R is ideal gas constant with 287 J/kg K, and $\overline{p}$and $\overline{T}$ are, respectively, the monthly mean pressure and temperature. Monthly mean air density at Younggwang was calculated with measurement data and it is presented in Fig. 13. Air density also shows larger vertical variation in winter compared to summer.

3. Potential power resource

3.1. Wind power density

The potential wind power density P available over a unit area normal to a wind of speed V is represented by

$$P = \frac{1}{2}\rho V^3 \tag{9}$$

The mean wind power density can be calculated using the measured data at each observation height by the following equation [13]:

$$\overline{P} = \frac{1}{2N}\overline{\rho}\sum_{i=1}^{N_{obs}} n_i V_i^3 \tag{10}$$

where $\overline{\rho}$ is the average air density for the given duration, V_i is the wind speed at the mid-point of the ith class, n_i is the frequency of occurrence in the ith class. Monthly mean power densities are calculated based on the time series of measurement of each month at height 26.31 and 97.35 m and presented in Figs. 14

and 15, respectively. At two elevations, the peak monthly power density was obtained in January.

In Fig. 16, the annually averaged power density and seasonally averaged values for winter were compared at each elevation. The annually averaged power density was obtained as 429 W/m^2 and the seasonal power density in winter was obtained as 510 W/m^2 at the top measurement elevation.

There are several classifications that indicate the qualitative evaluation of wind power density. Mirhosseini et al. [9] and Manwell et al. [17] introduced the following categories in terms of annual average wind power density:

- $\overline{P} < 100\ W/m^2$—low.
- $\overline{P} \approx 400\ W/m^2$—good.
- $\overline{P} > 700\ W/m^2$—great.

Another classification by the EWEA (European Wind Energy Association) for the wind power density is as follows [18]:

- $\overline{P} \approx 300–400\ W/m^2$—fairly good.
- $\overline{P} \approx 500–600\ W/m^2$—good.
- $\overline{P} \approx 700–800\ W/m^2$—very good.

According to the above criteria, the wind power in Fig. 16 presents a good condition for the construction of wind farm if the turbine hub height is above 46.31 m.

We also calculated $\overline{P}$ using the estimated seasonal Weibull models in Table 5 with the following relationship [7]:

$$\overline{P} = \int_0^\infty \frac{1}{2}\overline{\rho}V^3 f(V)\,dV = \frac{1}{2}\overline{\rho}c^3\Gamma(1+3/k) \tag{11}$$

For annual and winter distributions, the power density calculated from Eqs. (10) and (11) is compared at each measurement elevation, and their absolute errors are presented in Table 6 which shows that the estimated Weibull distribution accurately estimates the power density from real distribution of measurement.

Table 6
Estimated wind power density from measurement and fitted Weibull model (W/m^2).

Height	2011			2011—winter		
	Measure.	Weibull	Err.	Measure.	Weibull	Err.
26.31	276.82	272.06	4.76	384.61	385.79	1.18
46.31	315.82	313.36	2.46	400.85	401.88	1.03
56.31	337.73	340.00	2.27	413.15	415.19	2.04
66.31	380.22	383.33	3.10	464.99	466.35	1.37
76.31	371.07	374.18	3.12	440.51	442.14	1.63
86.31	384.42	389.57	5.15	452.27	453.98	1.71
96.31	407.03	417.02	9.99	484.62	489.37	4.75
97.35	429.20	437.86	8.67	509.97	512.58	2.61

3.2. Wind turbine production

For a given probability density function of the wind speed and turbine power curve, $P_t(V)$, the average wind turbine power $\overline{P}_t$ is obtained from

$$\overline{P}_t = \int_0^\infty P_t(V) f(V)\,dV \tag{12}$$

With a summation over N_B, the number of bins, the following expression, can be used to find the average wind machine power $\overline{P}$ [9]

$$\overline{P}_t = \sum_{i=1}^{N_B} \frac{1}{2}(V_{i+1}-V_i)\left[f(V_{i+1})P_t(V_{i+1})+f(V_i)P_t(V_i)\right] \tag{13}$$

In the following, some kinds of commercial offshore wind turbines are selected which have nominal power higher than 3.0 MW and available hub height near 97.35 m, to evaluate the net energy production at Younggwang region. Six wind turbines selected for the comparison are presented in Table 7 along with their rated power and other characteristics. All six selected are horizontal-axis, variable speed wind turbines with pitch control.

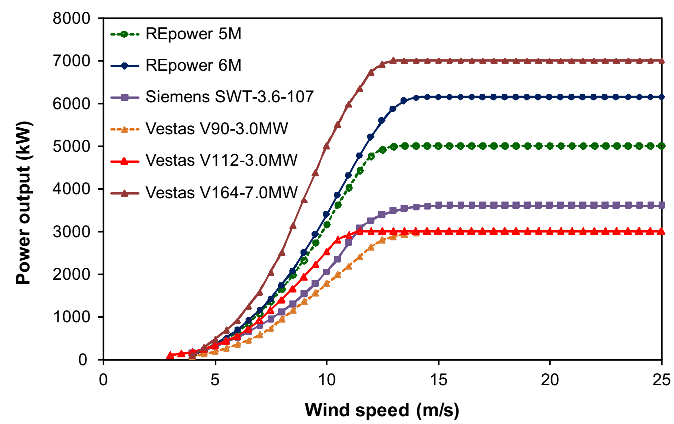


Fig. 17. Power curves of selected machines.

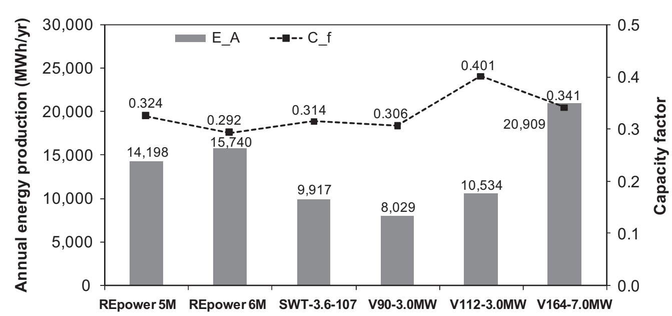


Fig. 18. Annual energy production and capacity factor of selected machines in 2011.

Table 7
Characteristics of selected wind turbines.

Model	Rated output (kW)	Diameter (m)	Hub height (m)	Cut-in wind speed (m/s)	Rated wind speed (m/s)	Cut-out wind speed (m/s)	Class (IEC)
REpower 5 M	5000	126	90–100	3.5	13.5	30	IB
REpower 6 M	6150	126	85–95	3.5	15	30	IB
Siemens SWT-3.6-107	3600	107	80–96	3–5	13–14	25	IA
Vestas V90-3.0 MW	3000	90	84–119	3.5	15	25	IIA
Vestas V112-3.0 MW	3000	112	84–119	3	12	25	IIA
Vestas V164-7.0 MW	7000	164	Site specific	4	13.5	25	S

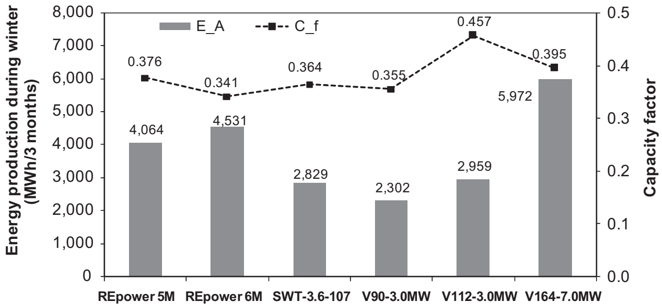


Fig. 19. Seasonal energy production and capacity factor of selected machines in 2011—winter.

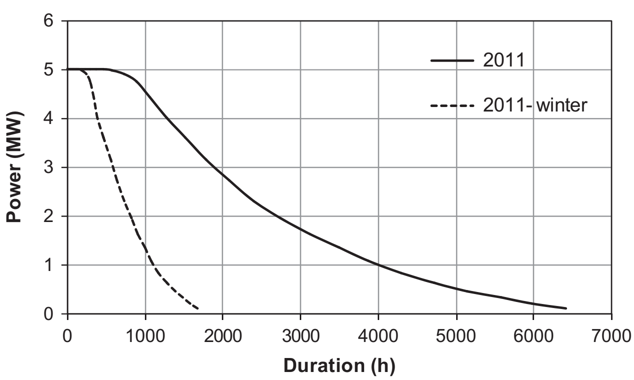


Fig. 20. Duration curves of REpower 5 M.

The pitch control system is one of the most widely used control techniques to regulate the output power of a wind turbine generator. The method relies on the variation in the power captured by the turbine as the pitch angle of the blades is changed. At wind speeds below the rated power of the generator, the pitch angle is at its maximum though it can be lower to help the turbine accelerate faster. Above the rated wind speed, the pitch angle is controlled to keep the generator power at rated power by reducing the angle of blades.

Among the selected turbine, Siemens' SWT 3.6-107 and Vestas V90 are established models in the offshore wind turbine market, whose total installed capacity is 270 and 290 MW, respectively [19]. A 3 MW-level turbine has been the leading large capacity models until recently. However, due to the recent developments in large capacity wind turbines, higher rated turbines such as the REpower 5 M/6 M are expanding their market share rapidly. Furthermore, the latest technical progress in offshore turbines has led to the commercialization of machines with enlarged capacity, such as Vestas' new V-164-7.0 MW launched in March, 2011. Design parameters for wind class provided by IEC [20] of each selected turbine are also presented in Table 7. Because 50 yr extreme wind speed around Younggwang was estimated 39.8 m/s [21], wind turbine class upper than class II is possible to use in this site.

The wind observation data at 97.35 m was selected for the assessment of the net energy production using Eq. (12). Power curves of each turbine are presented in Fig. 17. The net energy production E_A for a given duration T, 365 days for an year and 90 days for winter season, is obtained by using the following equation [22];

$$E_A = \overline{P}_t T \tag{14}$$

The capacity factor C_F is also an important index in measuring the productivity of a wind turbine. It compares the actual power production of a turbine over a given time duration with the amount of power of the turbine operated at the rated output for the same time duration [10,22]

$$C_F = \frac{E_A}{E_R} \tag{15}$$

where $E_R(=P_R T)$ is the maximum power of the turbine operating at the rated output P_R for time duration T.

The net energy production of each turbine and its capacity factor during 2011 and winter of 2011 is presented in Figs. 18 and 19. At least 8000 MWh/yr of energy production is possible by using one of the listed wind turbines in Table 7. During winter, we can expect at least 4000 MWh of energy production using wind turbine with output higher than 5 MW.

Because the master plan of the wind farm in the Younggwang determined to install 5 MW class wind turbines to be tied in a plant, the energy production by Repower 5 M turbine was selected to be analyzed in detail. The power duration curve is useful for comparing the energy potential by choosing the wind turbine type. It is a graph with the power output of a specific turbine on the y-axis and the number of hours in the given time duration for which the speed equals or exceeds each particular value on the x-axis [17]. Fig. 20 shows the power duration curve of REpower 5 M obtained from the measurement wind data at an elevation of 97.35 m. Because the areas under the curves are proportional to the available wind energy, the proportion of the energy potential in winter compared to annual production is visually apparent in this power duration curve. The time duration for this turbine to maintain the output as higher than 3 MW is about 550 h in winter, which is about 31% of annual time duration for output higher than 3 MW.

As we introduced the plan for wind farm around Younggwang region, it is planned to be installed about 500 machines with 5 MW capacity for the future construction of 2500 MW-level wind farm. For REpower 5 M, about 810 MW ($\overline{P}_t \times 500$) of annually averaged energy supply is expected for the complete wind farm with 2011 wind data. During the winter of 2011, 940 MW of energy supply by 500 machines of Repower 5 M was estimated. As a result, the completed wind farm is expected to provide about 12% of the peak electric demand in winter, and increases the electric power reserve rate by 1.3% in terms of 2011 electricity supply condition; the maximum electric demand of 73,140 MW in January 2011. The total annual energy production in this wind farm is expected to be 7096 GWh/yr.

4. Conclusion

In this research, the offshore wind energy potential of the wind farm, which is planned to be set up in Younggwang located on the west coast of the Korean peninsula, was evaluated. For the assessment, measurement data of 2011 from a meteorological mast called HEMOSU-1 are obtained; installed at 127° 07′ 45.30″ E and 35° 27′ 55.17″ N, a location of offshore near Younggwang:

(1) The annual mean wind speed for this site is estimated to be 7.122 m/s at an elevation of 97.35 m, which is relatively much stronger than the mean wind speed for any onshore location in Korea.
(2) The Weibull probability distribution was estimated from the frequency distribution of measurement data at each observation elevation and statistically significant results were obtained.
(3) From the measurement data, it was observed that the north-northwestern wind direction is prevalent due to the winter monsoon.

(4) Vertical profile of annually averaged data at Younggwang was linearly approximated by the power law with power of $\beta = 0.111$.
(5) The assessment of the available power density at 97.35 m indicates that there is a high wind power density averaged to be 429.20 W/m^2 annually and 509.97 W/m^2 during winter. This agrees well with the value obtained from the Weibull parameters' investigation.
(6) Among the selected commercial wind turbines with rated power in the range of 3–7 MW, REpower 5 M was analyzed in terms of the power duration curve. The results showed that the expected annual energy production will be about 7096 GWh/yr when the construction of the wind energy farm is completed as planned.
(7) Based on the maximum electric demand of 73,140 MW in January 2011, the completed wind farm is expected to cover 12% of peak demand and increase the electric power reserve rate by about 1.3% in the winter season.

Acknowledgments

This work is the outcome of a Manpower Development Program for Marine Energy by the Ministry of Land, Transport and Maritime Affairs(MLTM) and a study on the demonstration project for 2.5 GW offshore wind farm at the southern part of yellow sea by the Ministry of Knowledge Economy(MKE).

References

[1] Kim JY, Kang KS, Oh KY, Lee JS, Ryu MS. Assessment of possible resources and selection of preparatory sites for offshore wind farm around Korean Peninsula. Journal of the Korean society for new and renewable energy 2009;5(2):39–48 in Korean.
[2] Warner TT, Kuo YH, Doyler JD, Dudhia J, Stauffer R, Seaman NL. Nonhydrostatic, meso-beta-scale, real-data simulations with the Penn State University/ National Center for Atmospheric Research mesoscale model. Meteorological Atmospheric Physics 1992;49:209–27.
[3] European Environment Agency. Europe's onshore and offshore wind energy potential: an assessment of environmental and economic constraints, EEA technical report no. 6/2009. European Environment Agency; 2009.
[4] Kang KS, Lee JS, Kim JY, Ryu MS. Economic analysis of offshore wind farm considering domestic development conditions of Korea. Journal of Wind Energy 2011;2(1):37–43 in Korean.
[5] Ahmed Shata AS, Hanitsch R. The potential of electricity generation on the east coast of Red Sea in Egypt. Renewable Energy 2006;31:1597–615.
[6] Ahmed Shata AS. Wind energy as a potential generation source at Ras Banas, Egypt. Renewable and Sustainable Energy Reviews 2010;14:2167–73.
[7] Dahmouni AW, Ben Salah M, Askri F, Kerkeni C, Ben Nasrallah S. Assessment of wind energy potential and optimal electricity generation in Borj-Cedria, Tunisia. Renewable and Sustainable Energy Reviews 2011;15:815–20.
[8] Fyrippis I, Axaopoulos PJ, Panayiotou G. Wind energy potential assessment in Naxos Island, Greece. Applied Energy 2010;87:577–86.
[9] Mirhosseini M, Sharifi F, Sedaghat A. Assessing the wind energy potential locations in province of Semnan in Iran. Renewable and Sustainable Energy Reviews 2011;15:449–59.
[10] Mostafaeipour A, Sedaghat A, Dehghan-Niri AA, Kakantar V. Wind energy feasibility study for city of Shahrbabak in Iran. Renewable and Sustainable Energy Reviews 2011;15:2545–56.
[11] Justus CG, Mikhail A. Height variation wind speed and wind distributions statistics. Geophysical Research Letters 1976;3(5):261–4.
[12] Justus CG, Hargraves W, Garvine R. Methods for estimating wind speed frequency distributions. Journal of Applied Meteorology 1978;17:350–3.
[13] Ilinca A, McCarthy E, Chaumel JL, Retiveau JL. Wind potential assessment of Quebec Province. Renewable Energy 2003;28:1881–97.
[14] Omer AM. On the wind energy resources of Sudan. Renewable and Sustainable Energy Reviews 2008;12:2117–39.
[15] Awanou CN, Degbey JM, Ahlonsou E. Estimation of mean wind energy available in Benin (Ex Dahomey). Renewable Energy 1991;1(5/6):845–53.
[16] Khogali A, Albar OF, Yousif B. Wind and solar energy potential in Makkah (Saudi Arabia)_comparison with Red Sea coastal sites. Renewable Energy 1991;1(3):435–40.
[17] Manwell JF, McGowan JG, Rogers AL. Wind energy explained: theory, design and application. Amherst, USA: John Wiley & Sons; 2002.
[18] Garrad A. Wind energy in Europe: a plan of action, summary report of wind energy in Europe-time for action. The European Wind Energy Association; 1991.
[19] Andreas T Concepts for high power wind turbines introducing HTS technology. In: World green energy forum, Gyeongju, Korea; 2010. p. 17–9.
[20] IEC. Wind turbines—part 1: design requirements. IEC 61400-1; 2005.
[21] Oh KY, Kim JY, Lee JK, Ryu MS, Lee JS. Wind resources assessment and performance evaluation of wind turbines for the test-bed of offshore wind farm. Journal of Wind Energy 2011;2(1):15–20 in Korean.
[22] Chang T-J, Wu Y-T, Hsu H-Y, Chu C-R, Liao C-M. Assessment of wind characteristics and wind turbine characteristics in Taiwan. Renewable Energy 2003;28:851–71.